Surface Segregation of Polyethylene in Low-Density Polyethylene/Ethylene–Propylene–Diene Rubber Blends: Aspects of Component Structure

Dariusz M. Bieliński,[1] Łukasz Kaczmarek[2]

[1]*Institute of Polymer and Dye Technology, Technical University of Łódź, Łódź, Poland*
[2]*Institute of Materials Engineering, Technical University of Łódź, Łódź, Poland*

Received 20 October 2004; accepted 2 July 2005
DOI 10.1002/app.23379
Published online in Wiley InterScience (www.interscience.wiley.com).

ABSTRACT: Aspects of the molecular weight and its distribution, the branching of low-density polyethylene (LDPE), and the molecular composition of the ethylene–propylene–diene rubber (EPDM) matrix are presented in this article in terms of their influence on the surface segregation of polyethylene (PE) in elastomer/plastomer blends. All of the PEs studied, despite different weight-average molecular weights and degrees of branching, segregated to the surface of the LDPE/EPDM blends. Atomic force microscopy pictures demonstrated defective crystalline structures on the surface of the blends, which together with a decrease in the degrees of their bulk crystallinity and a simultaneous increase in their melting temperatures, pointed to a low molecular weight and a defective fraction of PE taking part in the surface segregation. The extent of segregation depended on the molecular structure of the EPDM matrix, which determined the miscibility of the components on a segmental level. The higher the ethylene monomer content in EPDM was, the lower was the PE content in the surface layer of the blends. The composition and structure of the surface layer was responsible for its lower hardness in comparison with the bulk of the blends studied. The surface gradient of the mechanical properties depended on the physicochemical characteristics of the components and the blend composition, which created the possibility of tailoring the LDPE/EPDM blends to dedicated applications.
 J Appl Polym Sci 100: 625–633, 2006

Key words: atomic force microscopy (AFM); blends; indentation; polyolefins; surfaces

INTRODUCTION

Much attention has been paid recently to materials based on polyolefins, such as polyethylene (PE), polypropylene, and copolymers or terpolymers of their monomers [ethylene-propylene rubber (EPM) or ethylene–propylene–diene rubber (EPDM), respectively], because of their versatile properties, including low cost, easy processing, accessibility of the components, high strength-to-density ratio, corrosion resistance, and biocompatibility.[1] Nevertheless, an extended field of application often demands that different types of polymers be blended to meet various kinds of processing requirements and final properties.[2–4] Altering the content or structure of polyolefins for blending with EPDM makes it possible to produce a wide range of engineering elastic materials of different mechanical characteristics and tribological properties.[5–7]

One can shape the properties of the materials through their adequate composition and by applying knowledge on the influence of the morphology of the crystalline phase, the degree of branching, and the molecular weight of the polyolefins on the blend structure.[8,9] Blends perform well in a wide range of applications for which their individual components are not suitable. Apart from structural changes, modifications in the surface layer of rubber have been detected, namely, migration and surface segregation in the polymer system. The migration and blooming of low-molecular-weight substances is well known in polymer technology,[10,11] whereas the surface segregation of polymeric components of their blends has seldom been presented in the subject literature.[5,12]

In multicomponent polymer systems, phase separation occurs very often. Polymers are generally immiscible from a thermodynamic point of view. In many cases, separation is realized by surface segregation, which is a function of the physical properties of the compounds being blended and the conditions of processing. On the one hand, it depends on the chemical composition, molecular structure, and degree of crystallinity (X_c) of the components, but on the other hand, it can be influenced by the temperature of mixing, cooling rate, and energetic characteristics of a mold.[13–15] The surface segregation taking place in polymer blends produces a gradient structure, where the concentration of one component gradually

Correspondence to: D. M. Bieliński (dbielin@mail.p.lodz.pl).

TABLE I
Physical Characteristics of the Polymers

Polymer	Density (g/cm^3)	Solubility parameter $(J^{0.5}/m^{1.5})^{16}$	Degree of branching[a] (CH_3 at 100°C)	X_c[b]	T_m(°C)	M_w	M_w/M_n
EPDM1	0.86	15.9×10^{-3}	—	3.9	—	—	—
EPDM2	0.86		—	1.1	—	—	—
EPDM3	0.86		—	0.0	—	—	—
LDPE1	0.920	15.4×10^{-3}	3.5	53.6	92	40,000	2.36
LDPE2	0.930		3.8	61.4	112	15,000	2.32
LDPE3	0.906		6.0	32.0	90	35,000	2.56

M_n = number-average molecular weight. EPDM1, EPDM2, and EPDM3 were Buna EPG-6470, G-2470, and G-3440, respectively (B); monomer composition by weight = 71, 69, and 48%, of ethylene; 17, 19, and 40% of propylene; and 1.2% of ethylideno-norbornene, respectively. LDPE1, LDPE2, and LDPE3 - were items 42.777-2, 42.778-0, and 42.779-9, respectively (Aldrich Chemicals, UK).

[a] Determined from IR spectra according to ref. [17].

[b] Calculated from the heat of melting as determined from DSC spectra.

changes from the surface to the bulk. The surface profile of the blend morphology is created. Knowledge of the nature of the segregation mechanisms makes it possible to design physicochemical depth profiles for the materials. A new generation of materials, tailor-made with properties exactly matching the exploitation requirements, can be created.

In this article, we describe the morphology, structure, and properties of polyolefin blends made of EPDM and low-density polyethylene (LDPE). The influence of the physical characteristics of both the EPDM matrix and the LDPE dispersed phase was studied. Special attention was devoted to the surface layer of the blends and related physical properties of the system.

EXPERIMENTAL

Materials

The polymers used in this study are listed in Table I, together with their physical characteristics. The method of blend preparation, at a temperature of 145°C, that is, well above the melting temperature (T_m) of the crystalline phase of PE, was described earlier.[5] Recipes for the mixes are given in Table II. They were designed in a way that enabled us to study the influences of the molecular structure of the rubber matrix and the molecular weight and crystallinity of the plastomer on the surface segregation of LDPE and the surface morphology of the LDPE/EPDM blends. Samples were steel-mold vulcanized in an electrically heated press under conditions determined rheometrically, according to ISO 3417.

TABLE II
Compositions of the Blends

No.	Component	Content (phr)
1	Elastomer (EPDM)	100.0
2	Plastomer (LDPE)	0.0–70.0
3	Dicumyl peroxide[a]	0.6

Vulcanization at 160°C for 30 min (ISO 3417).

[a] 95% purity, Merck Shuchardt (Germany).

The structural branching of the PEs studied was simulated from their ^{13}C-NMR spectra by application of Cherwell Scientific (Oxford, UK) NMR software. LDPE1 was pretty linear, containing statistically only one single carbon branch for every 90 carbons in the backbone. LDPE2 contained short branches, statistically every 80 carbons in the backbone. This time, every fourth branch was longer and constituted from 6 to 8 carbon atoms. LDPE3, the most branched of the polymers studied, contained short branches of 2–4 carbon atoms placed about every 15 backbone carbons.

Techniques

Gel permeation chromatography (GPC)

The molecular weights and their distributions for the PEs were measured with a Milipore Waters 150-C instrument (Milford, MA). The apparatus was operated at 142°C, with 1,2,4-trichlorobenzene as an eluent. Narrow-distribution polystyrene standards were applied for column calibration.

Differential scanning calorimetry (DSC)

The melting enthalpies (ΔH_m's) were determined with a NETZSCH 204 differential scanning calorimeter (Selb/Bayern, Germany) calibrated for temperature and enthalpy with an indium standard. Specimens of about 9–10 mg were frame cut from sheets with a constant thickness to eliminate the possible influence of specimen geometry on the shape of the DSC peaks. Experiments were carried out over the temperature

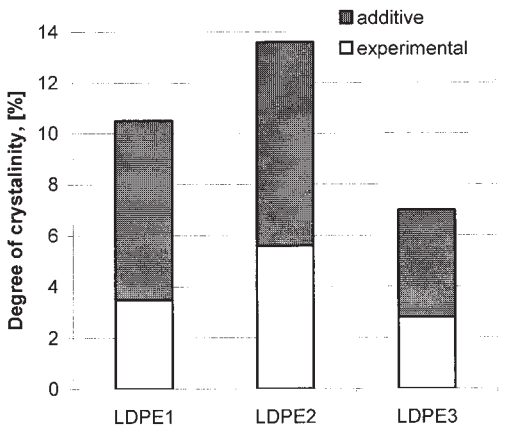

Figure 1 Comparison of X_c values for the 15-phr LDPE/EPDM3 blends, as calculated additively and derived from DSC spectra.

range 30–160°C. Before cooling, the samples were kept for 5 min at 160°C. Melting and crystallization were carried out at a scanning rate of 10°C/min. T_m and crystallization temperature (T_c) were taken as the temperatures corresponding to 50% of the adequate transition. ΔH_m and crystallization enthalpy were taken as the areas under the melting and crystallization peaks, respectively. The blend X_c was calculated from ΔH_m according to the following formula:

$$X_C = \frac{\Delta H_m}{\Delta H_m^0}$$

where ΔH_m^0 is the melting enthalpy of the polyethylene crystal (289 J/g).[18]

Fourier transform infrared spectroscopy (FTIR)

The samples were studied with a Bio-Rad 175C FTIR spectrometer (Krefeld, Germany) equipped with a Harrick horizontal attenuated total reflectance (HATR) or internal reflection spectroscopy attachment (Split Pea) over the wavelength range 600–4000 cm^{-1} under the following experimental conditions: 32 scans/resolution of 4 cm^{-1}. The use of these techniques provided the possibility for the depth profiling of the chemical compositions and supermolecular structures of the blends. The materials were probed with zinc selenide (ZnSe, $n = 2.4$, HATR), silicon (Si, $n = 3.9$, internal reflection spectroscopy), and germanium crystal (Ge, $n = 4.0$, HATR). Variation in the surface layer compositions of the LDPE/EPDM blends was studied, with the ratio of absorption peak intensities at 2850 and 2920 cm^{-1} applied, as suggested in the subject literature.[19] The depth of penetration, calculated for the previous wavelength region from Harrick's equation,[20] divided the experimental data into bulk, subsurface, and top surface data.

Atomic force microscopy (AFM)

AFM analysis was performed with a Metrology Series 2000 scanning probe microscope (Molecular Imaging, Tempe, AZ) operating in the contact mode. Si_3N_4 cantilevers with a resonance frequency of 20 kHz (Micro Mash, Tallinn, Estonia) were used. Phase images were recorded at scan speeds from 1 to 4 Hz. An area of 10 $\times$ 10 μm was scanned in respect to the surface geometry and tangential force.

Spherical indentation

A Nano Test 600 instrument (Micro Materials, Ltd., Wrexham, UK), equipped with a spherical stainless steel indenter with a radius (R) value of 5 μm was used for analysis of the hardness profile of the surface layers.[21] Tests were run within a depth-of-penetration range of 1000–8000 nm, with a loading rate of dP/dt of 0,02 mN/s. We calculated microhardness from the load-displacement data in the way proposed by Oliver and Pharr,[22] considering the slope of the unloading curves.

RESULTS AND DISCUSSION

When the phenomenon of surface segregation in polymer blends is discussed, questions on its origin and of its driving force arise. The answers seem to be complex, and despite many hypotheses, the explanations at this point in time remain controversial. Nevertheless, if one follows the behavior of low-molecular-weight paraffin analogues, it seems likely to be a function of the components' miscibility, specific interactions, and the ability of the polymers to crystallize.[23]

In the light of the previous discussion, we decided to check

1. What role in the surface segregation of LDPE in amorphous EPDM matrix was played by structure of the plastomer.

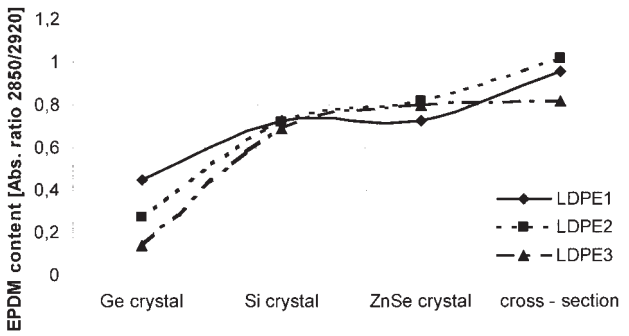

Figure 2 Elastomer content in the surface layer of the 15-phr LDPE/EPDM3 blends.

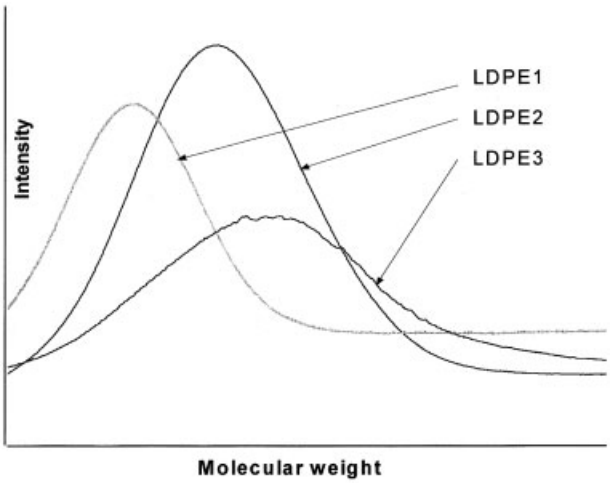

Figure 3 GPC curves of the molecular weight distributions for the PEs.

2. How the structure of the EPDM matrix influenced the surface segregation of PE.

Influence of PE structure on its surface segregation in an elastomer matrix

Figure 1 shows the values of X_c for a series of polyolefin blends. X_c values of the LDPE/EPDM blends derived from DSC measurements in each case were lower than those calculated additively, probably because the solubility parameters for both EPDM and LDPE were close to each other (EPDM = 15.9×10^{-3} and LDPE = 10.4×10^{-3} $J^{0.5}/m^{1.5}$, respectively[18]) and the mutual solubilization of the components on a segmental level took place during blending. This made it difficult for the crystalline phase of LDPE, which was made of low-molecular-weight chains and to some extent defective chains, to recrystallize in an amorphous rubber matrix, which caused a decrease in the X_c blend.

Bonnerup and Gatenholm[20] evaluated this possibility with the FTIR-attenuated total reflectance (ATR) technique for the determination of the surface layer composition of isotactic polypropylene/EPDM blends. They indicated a linear correlation between the ratio of the absorption bands at 2850 and 2920 cm^{-1} and EPDM content in the blends. Both the absorptions were, however, associated with the vibrations of —CH_2— groups. For this reason, it was difficult to separate the signals originating from the plastomer and the elastomer. Nevertheless, when we compared the value of the absorption ratio calculated for the spectra obtained with a Ge crystal (the surface layer) to the value calculated for the spectra determined with a Si (the subsurface layer) or ZnSe crystal (the bulk experiment), an enrichment in the surface layer of the blends with a plastomer was obvious (Fig. 2). This phenomenon was likely to be the result of the migration of a low-molecular-weight fraction of LDPE to the surface.[5] This depended on the degree of branching, X_c, and the molecular weight of PE.

The surface segregation of low-molecular-weight and practically branch-free LDPE (LDPE1), which could simulate the linear, oligomeric fraction of an industrial plastomer, is understandable. However, the surface segregation of a higher molecular weight LDPE [LDPE3; weight-average molecular weight (M_w) = 35,000] or the branched one (LDPE2) was also detected. We concluded that either the degree of branching of the latter PEs was too low to influence their diffusion or the polymers exhibited bimodal molecular weight distribution and contained a low-molecular-weight fraction (Fig. 3), which was even more likely. The GPC curve for LDPE3 presented the broadest M_w distribution among the PEs studied. The molecular weight distribution of LDPE3 was about 10% higher than LDPE1 or LDPE2. Generally, the most defective crystalline phase, swollen by an amorphous EPDM matrix, could not recrystallize afterward, and a

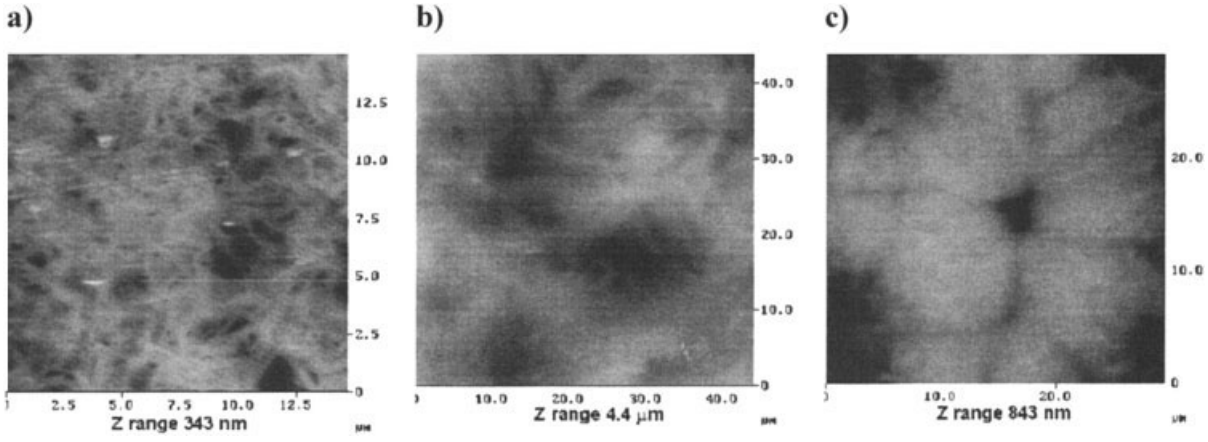

Figure 4 AFM pictures of the surfaces of the plastomer components: (a) LDPE1, (b) LDPE2, and (c) LDPE3.

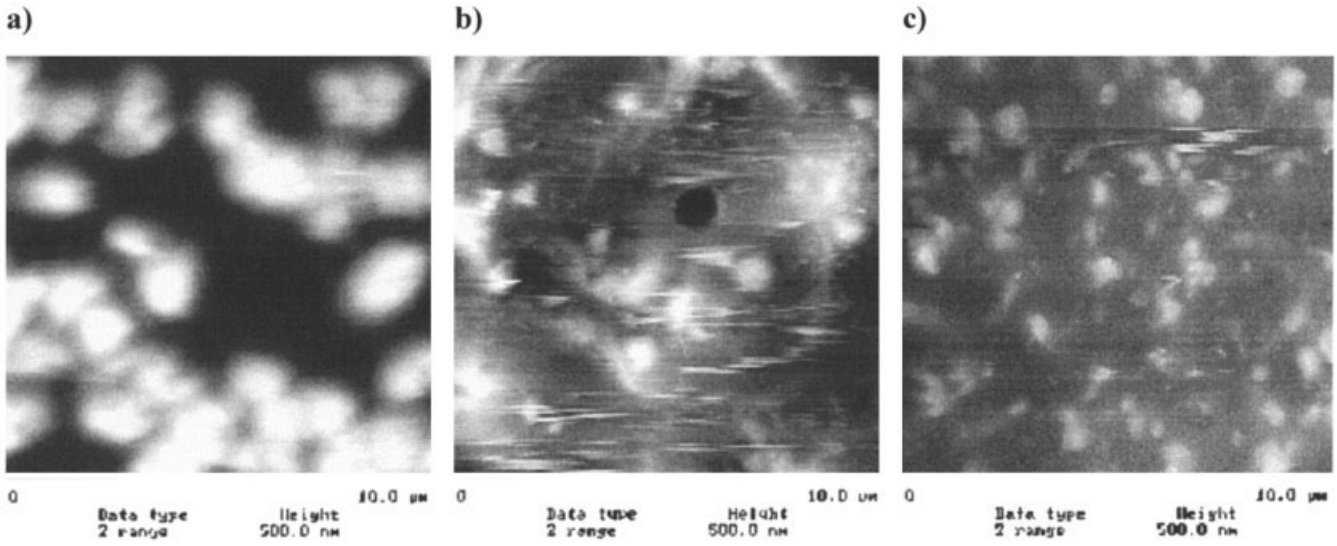

Figure 5 AFM pictures of the surfaces of the three LDPE/EPDM blends: (a) LDPE1/EPDM3, (b) LDPE2/EPDM3, and (c) LDPE3/EPDM3.

high discrepancy between the experimental crystallinity data and those calculated additively was apparent (Fig. 1). The highest effect was found for LDPE2 (the PE with the longest branches). The average molecular weight did not provide sufficient information on the nature of the polymer. For the PEs studied, their low-molecular-weight fractions could have facilitated the observed migration to the surface.

From AFM analysis, one can see a crystalline phase on the surface of the plastomers studied (Fig. 4). The crystalline structures were very well developed in the background of the amorphous phase of PE. Despite a significant surface microroughness, various morphologies of the crystalline phase for PEs could be recognized. The biggest, but to some extent defective, crystallites in the form of spherulites were present for LDPE2 (the plastomer with the highest X_c). The smallest crystallites were formed for LDPE1 (the plastomer with the lowest molecular weight). For LDPE3 (the plastomer with the highest molecular weight), also considerably big but also compact spherulites were visible. However, this time they were present in smaller numbers, which was in agreement with the calculations on crystallinity from the DSC spectra. AFM examination of the 15-phr LDPE/EPDM3 blends confirmed the surface segregation of an oligomeric phase of LDPE. Already, on first sight, it was possible to conclude that this phenomenon hardly depended on the degree of chain branching or on the molecular weight of the PEs studied (Fig. 5). The conclusion was in agreement with FTIR spectra. However, the AFM pictures of the blends' surfaces were different from those of the adequate PEs.

PE chains formed on the surface of the system's more or less defective crystalline phase. Such morphology (Fig. 5) may additionally indicate the heterogeneous nature of the surface segregation.[24] Low-molecular-weight chain fragments reptated toward the

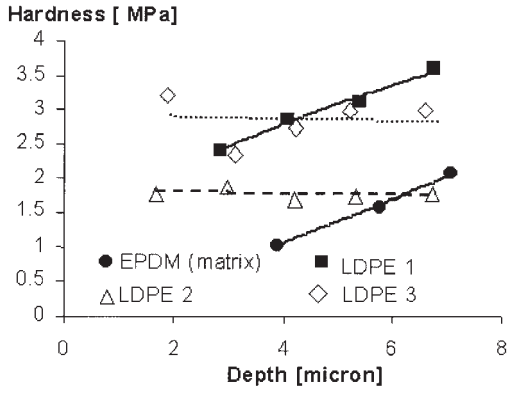

Figure 6 Microhardness profile of the surface layers of the of 15-phr LDPE/EPDM3 blends. The profile for the EPDM3 matrix is given for comparison.

TABLE III
Results of Thermal Analysis (DSC) for the LDPE 2/EPDM Blends

LDPE content (phr)	LDPE2/EPDM1		LDPE2/EPDM3	
	T_m (°C)	T_c (°C)	T_m (°C)	T_c (°C)
5	104	89	106	83
10	104	89	109	85
15	106	91	110	88
25	108	95	111	91
50	110	98	112	96
70	111	99	114	99
100	117	102	117	102

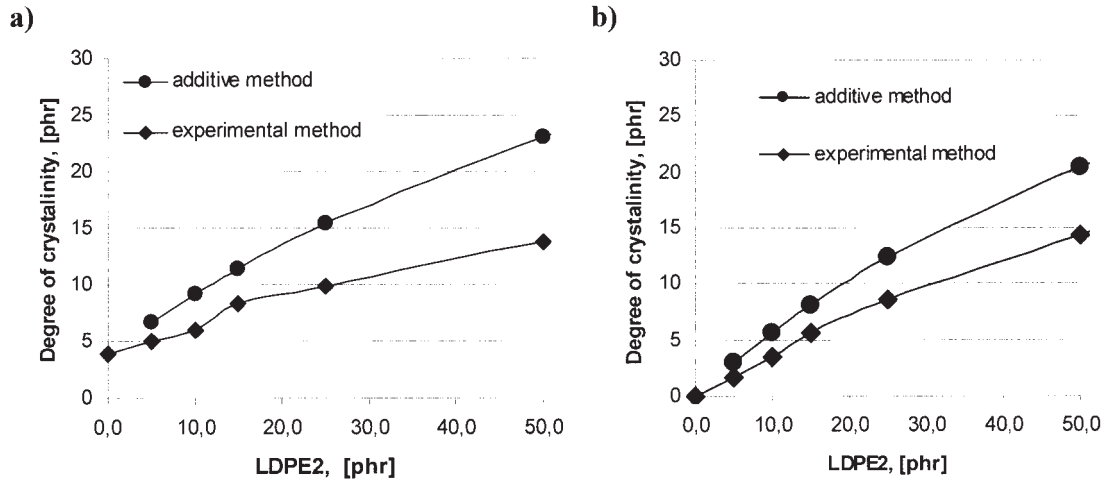

Figure 7 Comparison of X_c values for the LDPE2/EPDM blends, as calculated additively and derived from DSC: (a) LDPE2/EPDM1 and (b) LDPE2/EPDM3.

surface through less packed channels, formed in the EPDM matrix; thus, crystalline regions visible in the AFM pictures reflected the morphology of the blends. Crystallites visible on the surface were bigger when PE with a lower molecular weight was added, which seemed reasonable from the point of view of the possible dimensions and transport capability of the channels. Some deviations from this rule were present for the LDPE2 sample, that branching did not facilitate the surface segregation of the macromolecules. However, neighboring crosslinks between rubber macromolecules were placed every 10 to 100 carbon atoms,[25] so they practically could not interfere with the surface migration, even for LDPE2 molecules, which left the driving force of the phenomenon as the difference in the solubility parameters of the components and the ability of the PE phase for crystallization.[26] For example, on the surface of the LDPE1/EPDM3 blend, very thick crystals with average dimensions of 1 μm were formed. For PE, with LDPE3 blended with the same elastomer as before (EPDM3), there were crystals with average dimensions reaching up to about 2.5 μm. The correlation presented between the molecular weight of a plastomer, its X_c, and the surface morphology of its blend with rubber changed when the structure of the matrix changed. AFM pictures for the same PEs blended either with a sequenced elastomer (EPDM2) or a block elastomer (EPDM1) looked different from the pictures obtained for the system with an amorphous matrix (EPDM3). The influence of the rubber matrix on the surface migration of PE is discussed next.

The microhardness profiles of LDPE/EPDM blends containing EPDM3 (Fig. 6) provided more proof of the surface segregation of the oligomeric phase. From the spherical indentation data, we found that the addition

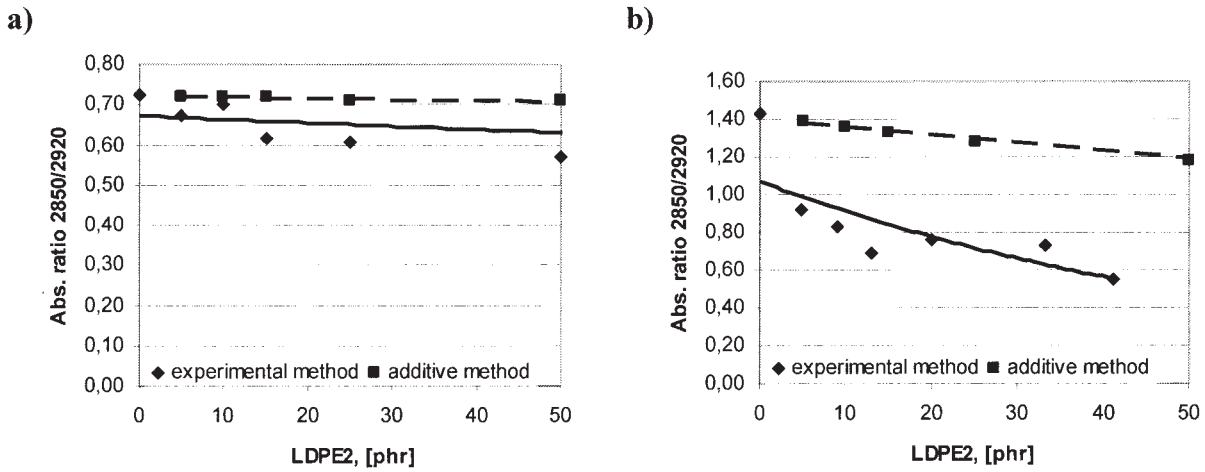

Figure 8 Comparison of data calculated additively and experimental data (derived from FTIR spectra) on the compositions of LDPE2/EPDM1 blends as a function of plastomer content: (a) LDPE2/EPDM1 and (b) LDPE2/EPDM3.

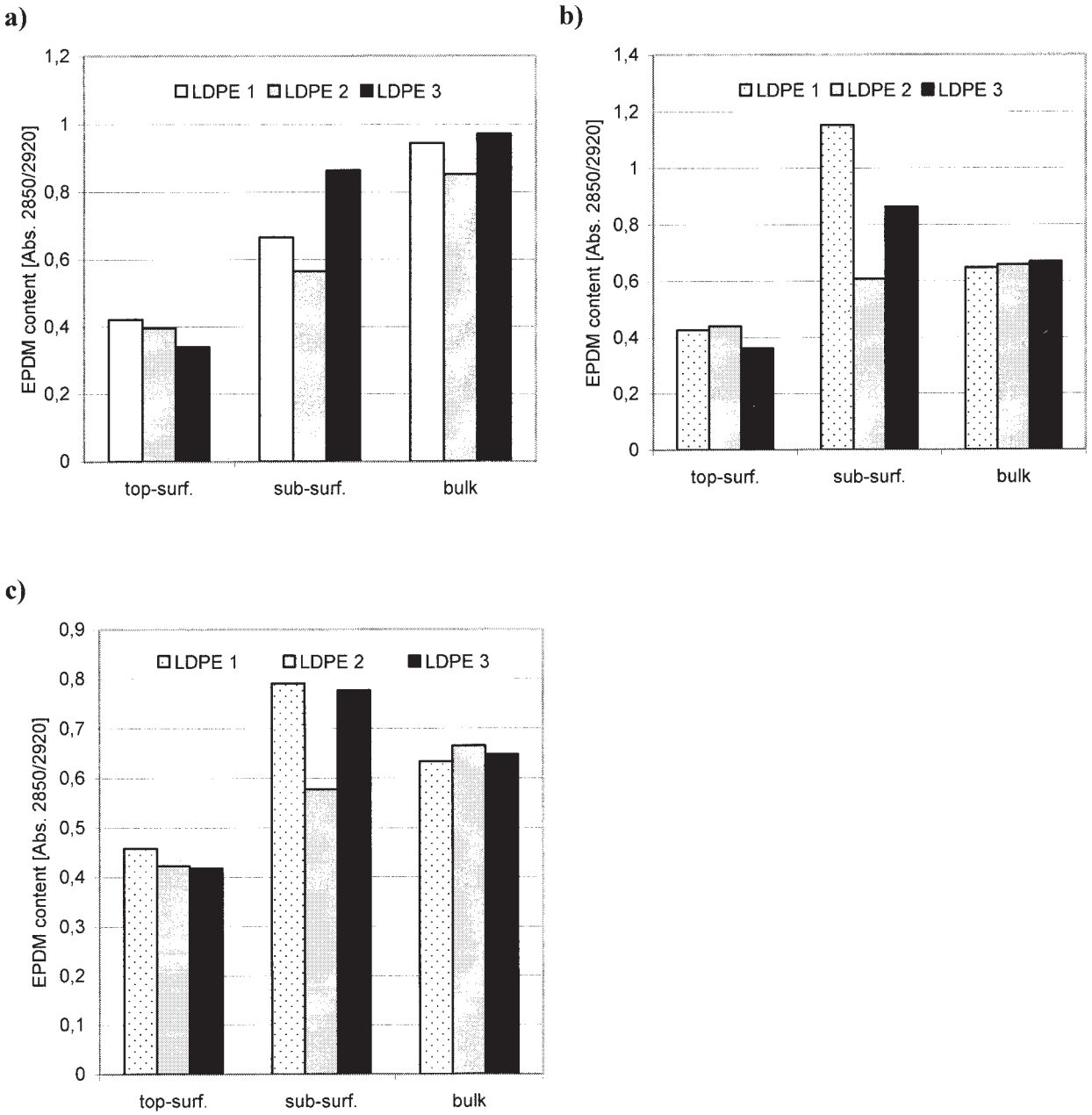

Figure 9 Profile of the surface segregation for the following blends: (a) LDPE2/EPDM1, (b) LDPE2/EPDM2, and (c) LDPE2/EPDM3.

of 15 phr LDPE increased the hardness of EPDM. However, the microindentation carried out on the sample cross-sections gave higher values compared to those of their surface layer. Some surface gradient of hardness was already visible for the linear LDPE1, which was the most prone to segregation. This observation was also in accordance with the analysis of the FTIR-ATR spectra. The degree and gradient of the surface plastification of EPDM by the migrating low-molecular-weight fraction of PE varied. However, no correlation between the hardness of the blends and the molecular weight of the plastomers was found. When the morphology of LDPE was compared to that of its blend with EPDM3, some deterioration of the crystalline phase organization was visible.

We concluded that the surface crystallites were more defective than crystals formed in the bulk. The low-molecular-weight fraction of LDPE migrating to the surface of blends could probably hardly recrystallize, even on the free surface. The crystallites formed were more defective, which together with the plastification of the EPDM matrix by the segregation of the low-molecular-weight plastomer phase, were responsible for the decrease in hard-

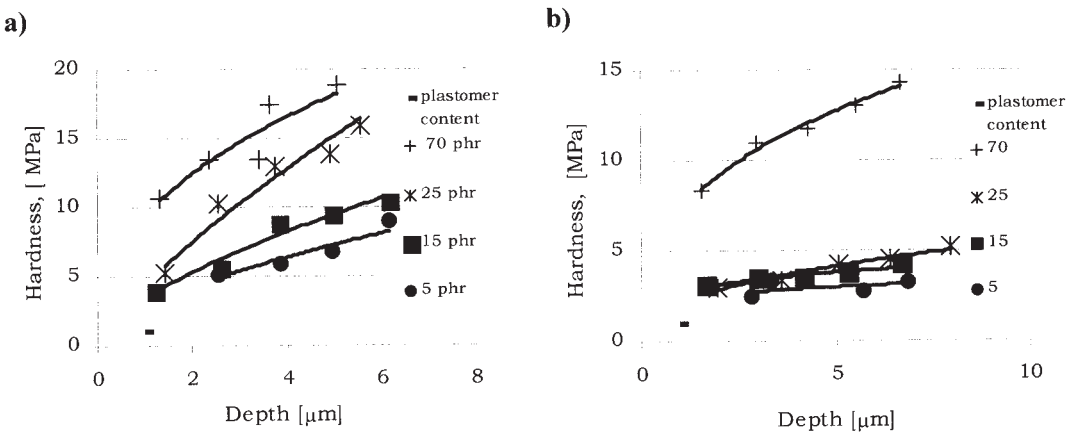

Figure 10 Profile of the hardness values for LDPE2/EPDM blends as a function of plastomer content: (a) LDPE2/EPDM1 and (b) LDPE2/EPDM3.

ness. The plastification effect increased closer to the surface of the system. The hardness of the LDPE/EPDM blends increased with increasing degree of plastomer crystallinity, no matter what the macromolecular structure of PE within the plastomers range was studied.

Influence of the elastomer matrix structure on the surface segregation of PE

Together with an increase in the propylene monomer content in the EPDM macromolecules, the mutual miscibility with PE on a segmental level decreased. The temperature of the phase transition of the blend was in an agreement with this result (Table III). T_m was slightly higher for the EPDM3 matrix system. On the other hand, a higher T_c was obtained for the blends containing the matrix with a block structure because of the easier crystallization of LDPE in the EPDM matrix enriched with long ethylene sequences able to cocrystallization. New recrystallized PE had a higher crystalline phase content but was less perfectly organized. This was the reason why it melted at a slightly lower temperature. On the other hand, blends containing an amorphous matrix exhibited higher T_m values. This time, the less ordered part of the crystalline phase of PE was swollen by the EPDM matrix, which caused the T_m of the purified crystallites to increase. This explanation is well illustrated by Figure 7, which presents discrepancies between those X_c values calculated additively and those determined experimentally.

Surface segregation took place for all of the blends under examination and did not depend on the macromolecular structure of the elastomer matrix within the range being studied. The results of the comparison between the blend compositions calculated additively and those determined experimentally from the FTIR spectra were in agreement with the previous conclusion (Fig. 8). A significantly bigger difference between curves, representing the relative rubber content, was observed for the amorphous matrix (EPDM3). This proves that together with an increase in the matrix X_c, the surface segregation decreased. However, in the case of LDPE/EPDM1 blends, a continuous increase in the plastomer content to the surface was observed [Fig. 9(a)]. A segregation profile does not depend on the molecular weight or the degree of branching of polyolefins studied. For the EPDM2 and EPDM3 matrices [Fig. 9(b,c)], the compositional gradient was shallower and exhibited a minimum LDPE content in the subsurface layer. This suggests that the PE phase present on the top surface came from the subsurface layer. The average content of LDPE in the top surface was almost two times that present in the subsurface layer.

From the microindentation data (Fig. 10), it follows that addition of the plastomer caused an increase in the hardness of the LDPE/EPDM blends in comparison to a nonmodified rubber. The same was demonstrated earlier for LDPE/EPDM3 blends (Fig. 6). The surface layer of blends again had lower hardness than their bulk. Following the previous discussion, we can explain this as a result of a lower crystallinity or the presence of more defective crystals being formed in the surface layer than in the bulk. The results of the micromechanical tests again were in agreement with the AFM pictures. Both suggest that nearer to the surface, a more defective crystalline phase was created. The second possible reason is associated with the plastification of the rubber matrix by a low-molecular-weight fraction of the plastomer, which was not even able to recrystallize on the blend's surface. The plastification effect was higher closer to the surface of the analyzed system. Blends of the sequenced matrix exhibited a higher negative gradient of hardness of the surface layer than systems composed of statistic EPDM. Apart from this, we again confirmed that mi-

crohardness increased with increasing plastomer X_c. This means that composition of the surface layer was independent from the macromolecular structure of the rubber matrix for the range of EPDMs that were studied. Hardness increased with increasing plastomer content in the LDPE/EPDM blends, which was the result of an increase in the total degree of blend crystallinity.

CONCLUSIONS

The experimental data we have presented confirmed the surface segregation of PEs in the LDPE/EPDM blends:

1. The PEs LDPE1 and LDPE2, which simulated a low-molecular-weight fraction of engineering material, were expected to segregate on the surface, despite some degree of branching of the latter, whereas the behavior of LDPE3 (M_w = 35,000) was a surprise. Probably, short molecular branches of the plastomer, associated with its small diffusion cross-section, were responsible for the obtained results. Another factor behind the surface segregation of LDPE3 may have been its lower crystallization ability compared to LDPE1 or LDPE2. This came from the broad molecular weight distribution of the polymer. The structure of the crystalline phase created this time was more defective, which made the blend X_c lower and eventually facilitated surface segregation.
2. The extent of segregation observed for blends studied depended on the molecular structure of the rubber matrix, which determined the miscibility of components on a segmental level. The higher the ethylene monomer content was, the lower the plastomer content was in the surface layer of the blends.
3. The composition of the LDPE/EPDM blends also influenced the surface segregation of LDPE. With increasing LDPE content, the surface segregation in the LDPE/EPDM blends intensified.
4. The blend X_c determined experimentally was lower than that calculated additively. This can be attributed to either the solvation of the crystalline phase of LDPE by the matrix or difficulty in recrystallization of LDPE in EPDM. The latter factor depended on the composition and molecular structure of the rubber matrix.
5. The surface layer of LDPE/EPDM blends had a lower hardness value compared to EPDM and exhibited a hardness. AFM pictures revealed highly defective crystalline structures present on the blends' surface. This again confirmed that apart from the miscibility of the components, the efficiency of LDPE to segregate in the EPDM matrix was also effected by the ability of the plastomer to recrystallize.

The authors thank Bayer (Germany) for donating EPDM samples.

References

1. Shin, Y. W.; Uozumi, T.; Terano, M.; Nitta, K. Polymer 2001, 42, 9611.
2. Bartczak, Z.; Argon, A. S.; Cohen, R. E.; Weinberg, M. Polymer 1999, 40, 2331.
3. Hedenqvist, M.; Conde Brana, M. T.; Gedde, U. W. Polymer 1996, 37, 5123.
4. Kresge, E. N. Rubber Chem Technol 1991, 64, 469.
5. Bielinski, D.; Slusarski, L.; Wlochowicz, A.; Douillard, A. Compos Interface 1997, 5, 155.
6. Bielinski, D.; Wlochowicz, A.; Dryzek, J.; Slusarczyk, C. Compos Interface 2001, 8, 1.
7. Olayo, R.; Manzur, A.; Hector Liamas, J.; Escobar, A. Polym Bull 1998, 41, 99.
8. Tashiro, K.; Kobayashi, M. Polymer 1996, 37, 1775.
9. Slusarski, L.; Bielinski, D.; Wlochowicz, A., Slusarczyk, C. Polym Int 1995, 36. 261.
10. Pysko, L.; Glijer, T.; Parys, T. Kautsch Gummi Kunstst 1998, 11, 797.
11. Choi, S. S. J Appl Polym Sci 1999, 73, 2587.
12. Chen, C. Y.; Md, W.; Yunus, Z. W.; Chiu, H. W.; Kyu, T. Polymer 1997, 38, 4433.
13. Avalos, F.; Lopez-Manchado, M. A.; Arroyo, M. Polymer 1996, 37, 5681.
14. Fan, Z. J.; Williams, M. C.; Choi, P. Polymer 2002, 43, 1497.
15. Shanks, R. A.; Li, J.; Long, Y. Polymer 2001, 42, 1941.
16. Barton, A. F. M. Handbook of Solubility Parameters and Other Cohesion Parameters; CRC: Boca Raton, FL, 1981.
17. Bojarski, J.; Lindeman, J. Polyethylene; WNT: Warsaw, Poland, 1963; p 109.
18. Brandrup, J.; Immergut, E. H. Polymer Handbook, 3rd ed.; Wiley: London, 1989; Chapter 5.
19. Bonnerup, C.; Gathenholm, P. J Polym Sci Part B: Polym Phys 1993, 31, 1487.
20. Harrick, N. J. International Reflectance Spectroscopy; Wiley-Interscience: New York, 1967.
21. NanoTest User Guide; Micromaterials: Wrexham, United Kingdom, 2000. http://www.micromaterials.com.
22. Oliver, W. C.; Pharr, G. M. J Mater Res 1992, 7, 1564.
23. Bielinski, D.; Slusarski, L.; Boiteux, G.; Parasiewicz, W. In Proceedings of the 38th World Polymer Congress IUPAC Macro, Warsaw, Poland, July 2000; p 1175.
24. Bielinski, D. Kautsch Gummi Kunstst 2004, 57, 13.
25. Slusarski, L. Kautsch Gummi Kunstst 1992, 45, 705.
26. Bielinski, D.; Glab, P.; Slusarski, L.; Chapel, J.-P. J Appl Polym Sci 2002, 86, 3368.